Semiconductor Physics, Quantum Electronics & Optoelectronics, 2026. V. 29, No 2. P. 261-270.

Sensors

Effect of substrate material on the sensitivity of SPR sensor with a polytetrafluoroethylene coating to inert gas

G.V. Dorozinsky[1], Yu.V. Kolomzarov[1], K.P. Grytsenko[1], V.V. Romanchuk[1], H.V. Dorozinska[2], T.P. Doroshenko[1], A.V. Samoylov[1], A.A. Korchovyi[1], O.M. Strilchuk[1], R.V. Khrystosenko[1]

[1]*V. Lashkaryov Institute of Semiconductor Physics, NAS of Ukraine, 41, Nauky Ave., 03028 Kyiv, Ukraine,*
[2]*National Technical University of Ukraine "Igor Sikorsky Kyiv Polytechnic Institute", 37, Prospect Beresteiskyi, 03056 Kyiv, Ukraine*
[*]*Corresponding author e-mail: gvdorozinsky@ukr.net*

Abstract. The effect of the substrate material combined with a polytetrafluoroethylene (PTFE) overlayer on the sensitivity of optical sensors based on surface plasmon resonance (SPR) in the Kretschmann geometry has been investigated. The experiments were performed at a fixed excitation wavelength of surface plasmons using a gold plasmon-supporting layer. The testing of the sensor elements was carried out by cyclic displacement of ambient air by inert helium in the flow cell. A comparative analysis of the characteristics of SPR sensors on substrates made of F1 optical glass and styrene-acrylonitrile (SAN) polymer was carried out in both the presence and absence of a PTFE overlayer on the gold film surface. It was established that replacing the glass substrate with the polymer (SAN) causes an increase in sensitivity from 45.8 to 48.1 deg/RIU due to a decrease in the refractive index; however, it doubles the figure of merit (FOM) from 26.2 to 50.1 RIU^{-1}. The application of the PTFE overlayer for both sensor types led to an increase in sensitivity: from 45.8 to 74.4 deg/RIU for the glass substrate, and from 48.1 to 52.1 deg/RIU for the polymer substrate. In addition to enhanced sensitivity, the use of the polymer material allows for reducing the cost of the final product, simplifying the stages of precision surface treatment. An additional advantage is the narrowing of the resonance curves, which significantly improves the accuracy of the resonance angle registration.

Keywords: sensor, surface plasmon resonance, substrate, polytetrafluoroethylene, styrene-acrylonitrile, helium, sensitivity, figure of merit.

https://doi.org/10.15407/spqeo29.02.261
PACS 42.79.Pw, 42.79.Qx, 73.20.Mf

Manuscript received 18.04.26; revised version received 02.06.26; accepted for publication 10.06.26; published online 23.06.26.

1. Introduction

In the modern world, there is a growing demand for highly accurate and sensitive sensor systems capable of real-time monitoring and control of various processes and conditions, which in turn drives the development of optical sensors. Optical sensors occupy an important position among contemporary analytical systems due to several significant advantages over other types of sensors, including electrochemical, amperometric, and semiconductor-based ones [1]. Unlike electrochemical sensors, they do not require direct electrical contact with the medium, which is particularly important when working with aggressive or biologically active substances. These include sensors based on the phenomenon of surface plasmon resonance (SPR). SPR technology opens up new possibilities for label-free analysis of biological and chemical objects in real time. In medicine, such sensors are used for early disease diagnosis and biomarker detection [2–4]; in immunology, SPR systems enable the investigation of specific antigen–antibody interactions [5]; in genetics, they allow the detection of DNA mutations [6]; and in veterinary science, they facilitate the rapid identification of infectious agents in animals [7]. In industry, these technologies are applied for quality control of products and technological processes [8, 9]. SPR sensors also play a crucial role in environmental monitoring, enabling the detection of harmful contaminants in air and water [10, 11].

Gas sensing is one of the key areas of modern science and technology, enabling air quality control, industrial process safety, and environmental monitoring [12]. Particular attention is paid to sensors based on the phenomenon of SPR, which are distinguished by high sensitivity and rapid response [13]. Due to the ability of SPR to respond to changes in the refractive index near a metal surface, these sensors can effectively detect even low concentrations of gases. Furthermore, advances in nanotechnology contribute to the improvement of SPR sensor designs [14, 15], enhancing their sensitivity and selectivity regarding specific gaseous substances. To achieve this, researchers have employed additional organic polymer layers such as calixarenes [16, 17], as well as metal oxides [18, 19]. In [19], the authors proposed an SPR sensor for n-hexane vapors incorporating an additional 20 nm zinc oxide layer fabricated using the sol–gel method [20], which exhibited four times higher sensitivity to *n*-hexane compared to the SPR sensor without the additional zinc oxide layer. The authors of [21] applied an SPR sensor for the detection of inert gases, specifically argon and helium; the limit of detection for the described sensor stood at $2.2\cdot10^{-1}$ RIU. Composite materials based on metal nanoparticles have also been widely explored. In particular, in [22], silver nanoparticles stabilized with branched polyethyleneimine (BPEI) and citric acid (CIT) were used as an active coating for SPR gas sensors. The authors demonstrated that these materials exhibit high sensitivity to ethanol and water vapors, while selectivity toward analytes depends on the nature of the organic coating. Based on the data presented in [22] and with account of the hydrophilic nature of the gold film surface, atmospheric moisture poses a significant challenge to the sensing element. The simultaneous adsorption of target molecules and water molecules from the air introduces substantial measurement errors. Consequently, utilizing a protective hydrophobic layer on the plasmon-supporting gold film serves as an effective approach to minimize moisture-induced interference during SPR sensor response measurements.

Polytetrafluoroethylene (PTFE) is a promising protective material for mitigating surface hydrophilicity. Due to its high thermal stability and chemical inertness, PTFE ensures the resistance of the sensor elements to moisture, which is a prerequisite for obtaining reliable and accurate measurement results. In SPR sensors, an additional PTFE layer has been used both as an intermediate layer between the prism and the metal to excite long-range surface plasmons [23] and as a top filtering layer for the separation of small molecules in aqueous solutions [24]. In our previous work [25], an SPR sensor for volatile compounds was proposed, incorporating an additional PTFE layer on an optical glass substrate (F1 grade, refractive index $n_D = 1.6128$) and a gold plasmon-supporting layer with a thickness of 50 ± 2 nm. It was demonstrated that the application of a PTFE film enhanced the sensor response for samples with PTFE layer thicknesses of 30 and 40 nm when exposed to saturated vapors of methanol, ethanol, acetone, and isopropanol, due to an increase in the effective interaction surface area. The highest response was observed for the sensing element with a 30 nm PTFE layer, showing nearly a three-fold increase in response to saturated acetone vapors compared to films without PTFE. Consequently, the PTFE overlayer has a dual purpose: providing a protective function and enhancing the sensor response.

Reducing the cost of SPR sensors, particularly regarding the sensing element, is another critical direction in their development. The vast majority of SPR sensors utilize optical glass as a substrate for the plasmon-supporting layer. However, optical glass is expensive due to stringent requirements regarding its optical characteristics and operations such as grinding and polishing. In addition, replaceable glass substrates with metal coatings are consumable components. Therefore, the transition to polymer substrates for SPR-based gas sensors represents a relevant direction for further development. For example, in [26], SPR sensor substrates made of optical polycarbonate ($n_D = 1.599$) were used, and SPR excitation in air was demonstrated; however, the sensing properties of such a sensor concerning gas environments were not investigated.

This study aimed to determine the effect of the substrate material with a PTFE overlayer on the sensitivity of the SPR sensor, and to evaluate the feasibility of utilizing polymer substrates for SPR sensors designed to detect gaseous substances, particularly inert gases.

2. Materials and methods

The object of this study comprised two types of sensing elements for SPR-based sensors with a gold plasmon-exciting layer. The first type consisted of a styrene-acrylonitrile (SAN) polymer substrate (with a refractive index of $n_D = 1.5663$) with and without an additional top PTFE layer. SAN was chosen as the substrate material due to its lower refractive index at the operating wavelength ($n_{650} = 1.5619$) compared to optical polycarbonate ($n_{650} = 1.5846$), since refractive index directly affects sensor sensitivity: the lower the substrate refractive index, the higher the sensor sensitivity, as shown in the work [27]. The SAN polymer has several key advantages over polycarbonate: it is significantly cheaper to manufacture, has higher resistance to aggressive chemicals (especially detergents, fats, and solvents), and exhibits less moisture absorption. The second type of sensing element was based on optical glass (F1 grade, $n_D = 1.6128$), also with and without an additional PTFE top layer. Both types of substrates were fabricated as thin plates with dimensions of 1×20×20 mm, with a tolerance not exceeding ± 0.1 mm. The surfaces of the glass substrates were mechanically polished to achieve a root-mean-square roughness ≤ 4 nm. *Prior to* deposition of the plasmon-supporting layer and the PTFE film, the glass substrates were cleaned in an ultrasonic bath using a 1:1 mixture of hydrogen peroxide and ammonium hydroxide, followed by rinsing with distilled water and air drying at room temperature. The polymer substrates were supplied with a protective film, which was removed immediately *prior to* metal deposition in vacuum.

A gold coating with a thickness of 48 ± 2 nm was deposited onto one side of the prepared substrate by thermal evaporation in vacuum using a VUP-5M system. Before deposition, the glass substrates were pre-coated with a 2…4 nm thick chromium sublayer to enhance the metal adhesion to the glass surface. The deposition process was carried out at a residual pressure of $(2…4)\cdot 10^{-3}$ Pa with a deposition rate of 5-6 nm/s. Real-time thickness control was ensured using a KIT-1 quartz crystal microbalance.

To form functional PTFE nanocoatings, the method of thermal evaporation of solid polymer particles in vacuum with additional electron activation was used [28, 29]. Deposition of 40-nm thick PTFE films was carried out using a modified UVN-74 vacuum system. The evaporation process was carried out with a specially designed water-cooled electron-beam evaporator–activator. The use of an activation current of 10 mA at an accelerating voltage of 0.8 kV enabled not only a stable deposition rate in the range of 2 to 4 nm/s, but also *in situ* electron activation of polymer fragments during evaporation.

The temperature regime was controlled at the evaporator, with a maximum heating temperature of 349 °C. Deposition was performed at a residual pressure in the working chamber of approximately $(1.7…2.5)\cdot 10^{-2}$ Pa ($(1.7…2.5)\cdot 10^{-4}$ mbar), which ensured a sufficient mean free path of particles toward the substrate and promoted the formation of a mesoporous film structure. In situ monitoring of film thickness and growth rate was carried out using a four-channel quartz crystal microbalance system (Sigma Instruments SQM-242). To ensure coating uniformity and to enable analysis of aggregation processes during film growth, a substrate holder rotation system was employed.

Surface microroughness was investigated using a NanoScope IIIa Dimension 3000™ atomic force microscope (Veeco Inc.). The scanning process was performed with silicon probes of the "Ultrasharp CSC38" series (Mikromasch, Germany), featuring a nominal tip radius of 10 nm. High resolution was ensured by the low noise level of the instrument (below 0.05 nm). The main structural parameters of the surfaces were calculated using the AFM data and Gwyddion 2.36 software.

The optical constants of the gold and PTFE films (refractive index n, absorption index k), as well as their thickness d, were determined based on the measured refractometric characteristics of the SPR for the investigated samples in ambient air.

The sensitivity S of the SPR sensor with different sensing elements was calculated according to the well-known relationship, defined as the ratio of the reflectance curve minimum shift $\Delta\theta$ (sensor response) to the refractive index alteration ΔN of the analyzed substance interacting with the sensing surface.

The refractometric characteristics of the investigated samples were measured using an SPR device Plasmon-6 (V. Lashkaryov Institute of Semiconductor Physics, NAS of Ukraine). The instrument implements the prism-based excitation of surface plasmons in the Kretschmann configuration [30]. The optical scheme of the sensor includes a semiconductor laser, a glass semipentaprism on which the investigated samples with a gold coating were placed, and a silicon photodetector. The wavelength of the semiconductor laser used for surface plasmon excitation was 650 nm. Angular dependences of the reflection coefficient were obtained by mechanical scanning through prism rotation, followed by determination of the resonance angle, defined as the minimum of the reflectance curve. The sensor response was recorded as the angular shift $\Delta\theta$ of the resonance minimum in the reflection characteristic, caused by changes in the refractive index ΔN of the analyzed medium. The operating angular range of the device is 38…69°, corresponding to refractive index measurements in the range of 1.00 to 1.41. Plasmon-6 can work with both gaseous and liquid media, so the range of measurement of the refractive index is as follows. The angular measurement range of the device for the excitation wavelength of surface plasmons λ = 650 nm specified in the article is limited by the optical geometry of the device. The angular resolution of the system is 3 arcseconds, which ensures the resolution at the determination of refractive index equal to $1\cdot 10^{-5}$.

Glass and polymer substrates coated with gold and with gold and PTFE layers, respectively, were mounted onto the working surface of a semi-pentaprism (made of K8 glass, n_D = 1.5141) of the Plasmon-6. Optical coupling between the substrate and the prism was ensured using an immersion liquid (microscope oil, n_D = 1.518, Merck). The refractometric characteristics were measured in the periodic resonance-angle scanning mode.

During the investigations, ambient air (n_D = 1.00028821 [31]) was utilized as a control gaseous medium, which was subsequently displaced by inert helium gas (n_D = 1.000034387 [31]) to alter the refractive index of the medium above the respective sensing element. Concurrently, the dispersion of the refractive index was considered to calculate ΔN, specifically: n_{650} = 1.00028738 [31] for air and n_{650} = 1.000034348 [31] for helium. It is understood that the values of the refractive indices for air and helium for a wavelength of 650 nm were used, which differ from those for a wavelength of 589.3 nm, for which the refractive index is most often indicated in tabular data. The displacement of air by helium resulted in a refractive index change of ΔN = –0.000253. The measurements were carried out using a flow cell hermetically mounted above the sensing element to ensure direct contact of air and helium with the PTFE or gold surface. The volume of each channel in the measurement flow cell was 50 µL. The delivery of the gases was maintained at a constant flow rate of 2 mL/min. The pumping of reagents was performed using a 10 mL syringe pump connected to the outlet of the cell. The inlet of the measurement flow cell was connected *via* a system of polymer tubing to reservoirs containing the corresponding inert gas.

The sensor response was calculated as the difference between the angular positions of the resonance minimum before and after adsorption. Based on the calculated sensor responses and the ΔN value, the sensitivity of the studied sensors was determined.

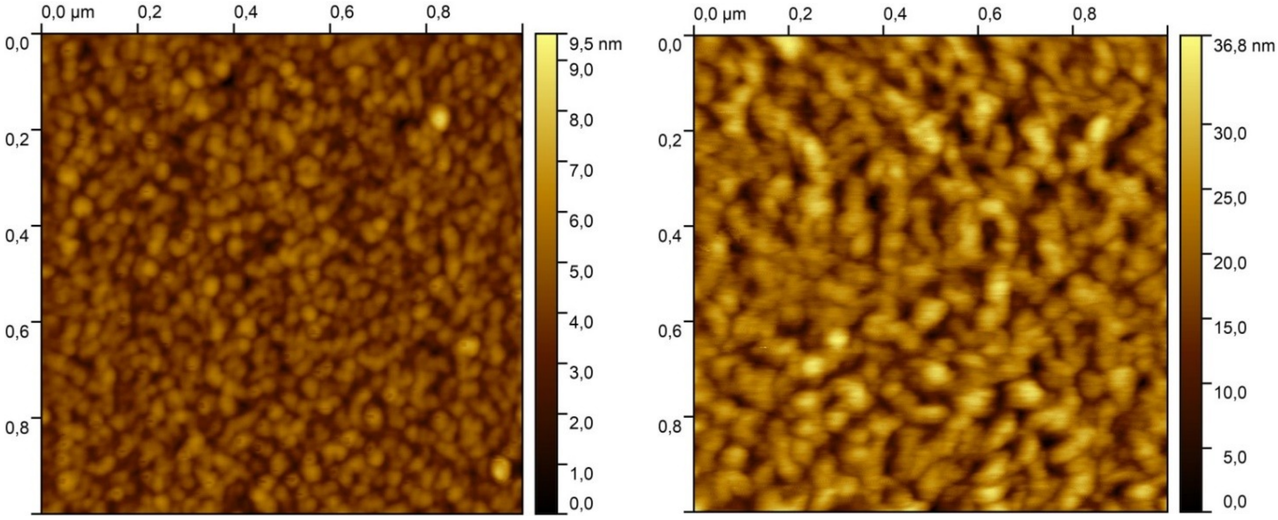

Fig. 1. AFM images of the surface for the glass substrate samples without covering (a) and with the 40-nm thick PTFE layer (b).

The measured refractometric characteristics were used to determine parameters such as the full width at half maximum (FWHM) of the resonance curve and the figure of merit (FOM = *S*/FWHM), which are widely applied in plasmonics for sensor benchmarking [32].

It should be noted that temperature fluctuations have a multifactorial influence on the physical parameters of SPR sensors [33] and also affect the vapor pressure of the investigated medium. In particular, both the real and imaginary parts of the dielectric functions of the sensor materials are temperature-dependent. Thus, thermal instability represents a significant source of measurement error.

To minimize temperature-induced errors in the Plasmon-6, the reservoirs containing the investigated media and the syringe pump were placed inside a thermostatic enclosure. Measurements were performed under standard environmental conditions: the temperature in the operation volume was 20 ± 0.2 °C, air humidity was 30 ± 1%, and atmospheric pressure was 740 ± 5 mmHg.

Similarly, fluctuations in atmospheric pressure were not considered: a variation of ± 5 mmHg results in a change in the refractive index of the medium at the level of $\pm 1 \cdot 10^{-7}$ RIU, which is two orders of magnitude lower than the sensitivity limit of the Plasmon-6.

3. Results and discussion

Fig. 1 presents AFM images showing the surface topology of the sensing elements on a glass substrate without an additional coating (a) and with a 40-nm thick PTFE layer (b).

From the analysis of the AFM images, the root-mean-square surface roughness R_{ms} over an area of 1 µm², the effective surface area A, the roughness parameter R_Z at 10 points along a baseline of 1.4 µm (image diagonal), and the arithmetic mean roughness R_a along the baseline, as well as the maximum statistical height (derived from the height distribution histogram) were determined (Table 1). The morphological analysis indicates that the deposition of the PTFE layer leads to a 3.6-fold increase in the root-mean-square roughness of the sensing element surface. This results in an increase in the effective interaction area with the analyzed medium and, consequently, an overall enhancement of the SPR sensor sensitivity.

Fig. 2 shows the measured refractometric characteristics, namely the dependences of reflection coefficient on the angle of incidence θ at the boundary between different media: metal on glass/air (F1_Au), metal on polymer/air (SAN_Au), PTFE on metal on glass/air (F1_Au_PTFE), and PTFE on metal on polymer/air (SAN_Au_PTFE).

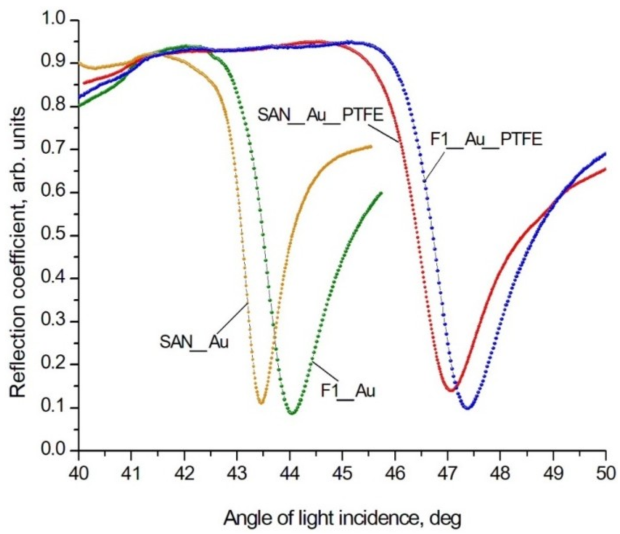

Fig. 2. Measured refractometric characteristics for the samples: SAN substrate with 48 nm gold film (SAN_Au), F1 glass substrate with 48 nm gold film (F1_Au), F1 glass substrate with gold film and additional PTFE layer (F1_Au_PTFE) and SAN substrate with gold film and additional PTFE layer (SAN_Au_PTFE).

Table 1. The calculated surface roughness and effective surface area from AFM images.

Structure type	d_{PTFE}, nm	R_a, nm	R_z, nm	R_{ms}, nm	A, μm^2
F1_Au	0.00	0.46	2.18	0.91	1.006783
F1_Au_PTFE	40.00	1.07	4.81	3.23	1.032824

Table 2. The calculated optical parameters of gold and PTFE layers on glass.

Structure type	Gold layer			PTFE layer	
	n	k	d, nm	n	d, nm
F1_Au	0.283	3.613	49.36	–	–
F1_Au_PTFE	0.254	4.172	46.84	1.353	43.47

Table 3. Results of measurements of sensor response and calculations of quality parameters of SPR-sensor.

Structure type	Δθ, arc.sec.	S, deg/RIU	FWHM, deg	FOM, RIU^{-1}	LOD, RIU
F1_Au	41.8	45.8	1.75	26.2	$10.9\cdot10^{-6}$
F1_Au_PTFE	67.8	74.4	2.08	35.8	$6.7\cdot10^{-6}$
SAN_Au	43.8	48.1	0.96	50.1	$10.4\cdot10^{-6}$
SAN_Au_PTFE	47.4	52.1	2.21	23.6	$9.6\cdot10^{-6}$

One can see that the measured resonance angle for the sensor with a SAN substrate (SAN-Au), compared to the resonance position obtained with the sensor with a glass substrate (F1-Au), is shifted toward lower angles, which is consistent with the data reported in [26]. A feature of Plasmon-6 is that the scanning angle cannot be greater than 18 degrees (12 degrees in the prism glass), so the authors chose the start of the scan of 40 degrees to demonstrate the critical angle, and therefore, the device could measure only up to 52 degrees. In Fig. 2, the angle is limited to 50 degrees, which was the authors' decision. This effect is explained by the decrease in the difference in refractive indices of the substrate and prism material when replacing F1 glass with the polymer. At the same time, the PTFE layer has a higher refractive index compared to both the F1 glass and SAN, so the presence of an additional PTFE layer leads to a shift of the resonance angle toward higher values by almost four degrees, from 43.5° to 47.2°. In this case, the resonance angle for the glass substrate is located at a larger value, namely close to 47.4°. The broadening of the resonance curve in the presence of the PTFE layer is associated with higher propagation losses of surface plasmons at the air-PTFE interface compared to propagation in air.

Using the refractometric curves and the special program package WinSpall 3.0, we calculated the optical parameters and thickness of gold and PTFE layers (Table 2).

The fitting considered the adsorption of moisture from the air onto the gold surface. The fitting results showed that moisture forms a heterogeneous water layer approximately 8 nm thick with an effective refractive index of 1.294. The lower value of the refraction index found for PTFE indicates inhomogeneity and porosity of the polymer layer. With the assumption that pores in the polymer layer are filled with air, and the refractive index of PTFE is $n = 1.375$ for a deposition residual pressure $2\cdot10^{-4}$ mbar in operation chamber [29], the porosity of these layers was calculated applying the simplified formula by Bruggeman [34]. According to the calculation results, the porosity value is 5.72%.

It is generally accepted that adsorption of gas molecules on the surface of the sensing element leads to a change in the dielectric permittivity of the near-surface layer, which in turn alters its refractive index and consequently causes a shift in the resonance angle. The kinetic profiles acquired using the Plasmon-6 are shown in Figs. 3 and 4, depicting the reflectance curve minimum shift due to the replacement of air by helium in the flow cell. The charts correspond to samples with various substrate configurations: glass substrate without PTFE (Fig. 3a), polymer substrate without PTFE (Fig. 3b), glass substrate with a PTFE overlayer (Fig. 4a), and polymer substrate with a PTFE overlayer (Fig. 4b). As can be seen, the sensor response is fully reversible, since the gas molecules do not undergo any chemical interaction with the surface. This confirms that the process is limited to physical adsorption of molecules on the surface layer.

The presented experiments demonstrate that the Plasmon-6 SPR instrument effectively detects the difference between air and helium. The sensitivity of the instrument to changes in the refractive index is highly elevated, and since inert gases are remarkably stable,

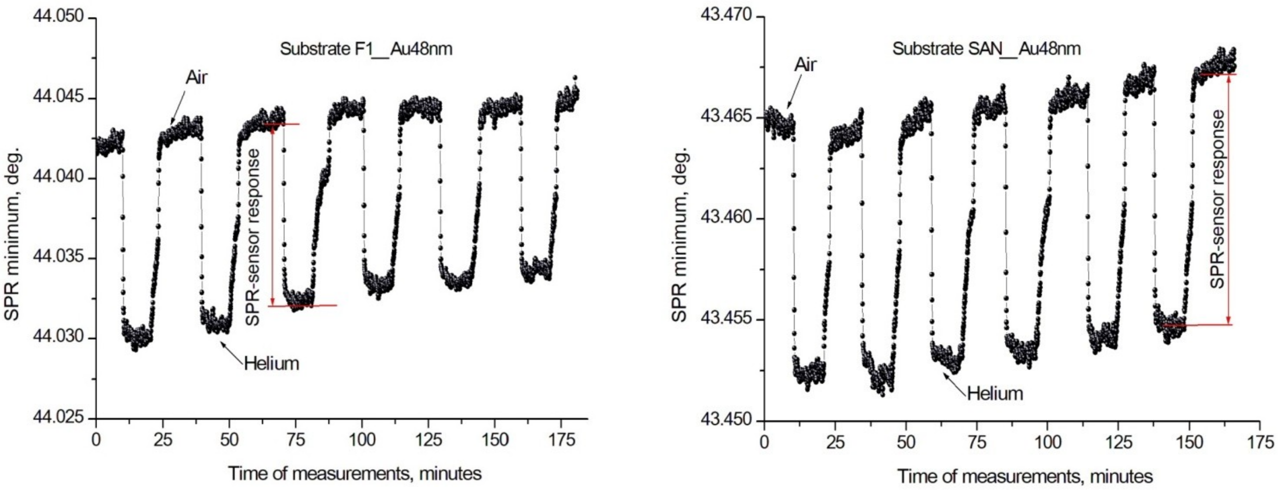

Fig. 3. The measured responses of SPR-sensors for glass (a) and polymer (b) substrates, when substituting the air in the flow-cell with helium.

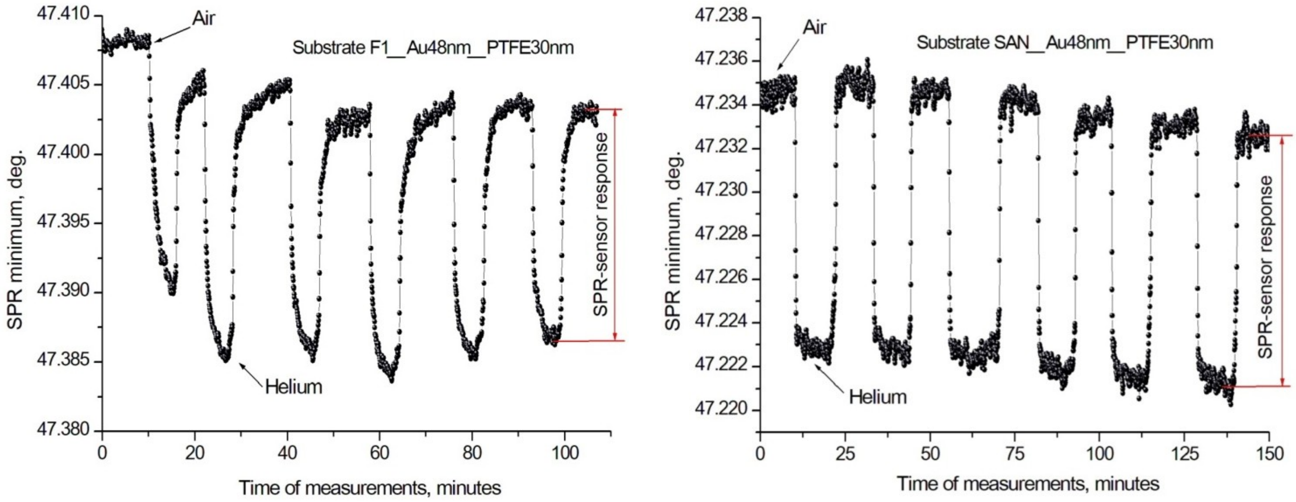

Fig. 4. The measured responses of SPR-sensors with an additional 40-nm thick PTFE layer for glass (a) and polymer (b) substrates, when substituting the air in flow-cell with helium.

the responses of the SPR minimum angle exhibit highly distinct plateaus with low noise levels. Consequently, this method holds great promise for measuring the refraction of inert gases.

To evaluate the statistical error of the analyte response measurement, a series of six air-to-helium substitution cycles was performed for each exchange of gases and sensor system, which allowed the maximum possible measurement uncertainty. The calculated mean sensor responses Δθ for different configurations, their sensitivity *S*, FWHM, and FOM, as well as the estimated limit of detection (LOD) are summarized in Table 3.

The sensitivity enhancement observed for both glass- and polymer-supported sensors upon applying the additional PTFE layer is attributed to an increased effective interaction area. This enhancement is driven by the higher surface roughness of PTFE (R_{ms} = 3.23 nm) relative to the bare gold surface (R_{ms} = 0.91 nm).

The substrate material also influences the efficiency of conductive heat transfer to the deposited film, thereby affecting its thermal formation regime. For F1 glass, thermal conductivity is almost an order of magnitude higher (0.71, 0.78 W/m·K for F2 as an analogue of the F1 brand [35]) than that of SAN polymer (0.085 W/m·K [36]). Therefore, PTFE films deposited on polymer substrates cool more slowly, which affects their structure, in particular porosity. This variation may account for the differences in the SPR sensor responses observed across distinct substrates: a less ordered structure on the glass substrate yields a higher response, thereby providing greater sensitivity. Consequently, for the sensor featuring a glass substrate with a PTFE overlayer, the responses exhibit a wider scatter in magnitude and a less pronounced plateau, indicating a gradual pore-filling process on the surface of the PTFE film. The resonance curve for the glass substrate was broader (FWHM = 1.75 deg) than that for the polymer substrate (FWHM = 0.96 deg) due to the presence of the chromium sublayer, which increased optical absorption. As a result, the highest FOM value was observed for the sensing element with the SAN substrate (50.1 RIU^{-1}), which was nearly twice as large as the FOM for the sensing element on the F1 glass substrate (26.2 RIU^{-1}). Thus, in terms of sensitivity, the SPR sensor with the glass substrate and a PTFE overlayer takes the lead, followed by the SPR sensor with the SAN substrate and PTFE. For the most sensitive sensor configuration, F1_Au_PTFE, a lower LOD can be achieved; factoring in the measured baseline noise level of the Plasmon-6 instrument ($5\cdot10^{-4}$ deg), it amounted to $6.7\cdot10^{-6}$ RIU. Meanwhile, for the polymer-based sensor SAN_Au_PTFE, the limit of detection was higher, reaching $9.6\cdot10^{-6}$ RIU.

Therefore, the research results demonstrate that transitioning to a polymer substrate is highly viable. Although the SPR sensor sensitivity remains largely unaffected, a clear economic benefit is achieved due to the lower cost of the substrate material and the simplified fabrication technology, which excludes substrate surface treatment. Furthermore, polymer substrate enables narrower resonance curves, thereby improving the accuracy of the resonance angle determination.

4. Conclusions

This study investigates the effect of the substrate material with a PTFE overlayer on the sensitivity of optical surface plasmon resonance (SPR) sensors operating in the Kretschmann configuration with a fixed excitation wavelength and a gold plasmon-supporting layer. Helium was used as the inert gas, which was alternately replaced by ambient room air inside the flow cell above the sensor sensing element. A comparative analysis was performed for SPR sensors utilizing F1 optical glass and SAN polymer substrates, both with and without a PTFE overlayer on the gold film surface. The experimental results demonstrate that using the polymer substrate slightly increased the sensitivity from 45.8 to 48.1 deg/RIU due to a lower refractive index, while simultaneously doubling the figure of merit from 26.2 to 50.1 RIU^{-1}. The application of electron-beam evaporation by using the modernized UVN-74 system enables the fabrication of PTFE films with a well-developed surface morphology (R_{ms} = 3.23 nm). Depositing the PTFE overlayer enhanced the sensitivity for both sensor types: from 45.8 to 74.4 deg/RIU for the glass substrate, and from 48.1 to 52.1 deg/RIU for the polymer substrate. More pronounced sensitivity enhancement observed for the glass substrate is attributed to its higher thermal conductivity, which influences the PTFE film formation process. Conclusively, the findings substantiate the feasibility of utilizing polymer substrates, which do not lead to a significant reduction in the sensor sensitivity. Concurrently, the polymer substrate provides substantial economic advantages due to lower material cost and a manufacturing process for the substrate surface treatment. Owing to the instrument high sensitivity to refractive index alterations and the exceptional stability of inert gases, the SPR minimum angle responses display clear plateaus characterized by low noise. Therefore, this approach represents a highly promising technique for the refractive index measurement of inert gases.

Acknowledgments

This work was supported by the National Academy of Sciences of Ukraine *via* the project “Creation of the latest functional materials and sensor elements for the needs of electronic and sensor technology” (No. III-3-2026, registration number: 0126U002776).

References

1. Lepore M., Delfino I. Optical sensors technology and applications. *Sensors*. 2022. **22**. P. 7905. https://doi.org/10.3390/s22207905.
2. Špringer T., Bocková M., Slabý J. *et al*. Surface plasmon resonance biosensors and their medical applications. *Biosens. Bioelectron.* 2025. **278**. P. 117308. https://doi.org/10.1016/j.bios.2025.117308.
3. Das S., Devireddy R., Gartia M.R. Surface plasmon resonance (SPR) sensor for cancer biomarker detection. *Biosensors*. 2023. **13**. P. 396. https://doi.org/10.3390/bios13030396.
4. Eshaghi G., Kaiser D., Rasouli H.R. *et al*. Highly sensitive and label-free detection of SARS-CoV-2 proteins *via* surface plasmon resonance using biofunctionalization with 1 nm thick carbon nanomembranes. *Sci. Rep*. 2025. **15**. P. 31248. https://doi.org/10.1038/s41598-025-16342-5.
5. Lisyte V., Kausaite-Minkstimiene A., Brasiunas B. *et al*. Surface plasmon resonance immunosensor for direct detection of antibodies against SARS-CoV-2 nucleocapsid protein. *Int. J. Mol. Sci*. 2024. **25**. P. 8574. https://doi.org/10.3390/ijms25168574.
6. Sobolevskyi M.S., Soldatkin O.O., Lopatynskyi A.M. *et al*. Application of modified gold nanoparticles to improve characteristics of DNA hybridization biosensor based on surface plasmon resonance spectrometry. *Appl. Nanosci.* 2023. **13**. P. 7521–7529. https://doi.org/10.1007/s13204-023-02930-2.
7. He J., Pan H., Feng L., Feng W. Dual-channel fiber-optic biosensors based on LSPR and SPR for the trace detection of rabies virus. *Appl. Phys. Lett*. 2025. **126**. P. 073701. https://doi.org/10.1063/5.0253941.
8. Granchak V.M., Sysjuk V.G., Dorozinska H.V. *et al*. Studying the polymerization efficiency of photo-sensitive compositions by surface plasmon resonance method. *SPQEO*. 2020. **23**. P. 393–399. https://doi.org/10.15407/spqeo23.04.393.
9. Hma Salah N., Pal A., Uniyal A. Enhancing precision in fuel adulteration detection: Utilizing a wavelength interrogation surface plasmon resonance approach. *Plasmonics*. 2025. **20**. P. 925–934. https://doi.org/10.1007/s11468-024-02340-2.

10. Chau Y.-F. Plasmonics in environmental sensing, pollution monitoring, and sustainable applications. *Mater. Today Phys*. 2026. **60**. P. 101984. https://doi.org/10.1016/j.mtphys.2025.101984.
11. Klestova Z., Yuschenko A., Blotska O. *et al.* Experimental and theoretical substantiation of the express method development for detection of enteroviruses in water by surface plasmon resonance method. *Innov. Biosyst. Bioeng*. 2019. **3**. P. 52–60. https://doi.org/10.20535/ibb.2019.3.1.163106.
12. So S.H., Lee S.Y., Kang H. *et al.* Metal-organic frameworks for gas sensors: comprehensive review from principal, fabrication to application. *Int. J. Extreme Manuf.* 2026. **8**. P. 012001. https://doi.org/10.1088/2631-7990/ae00a9.
13. Chauhan B.V.S., Verma S., Azizur Rahman B.M., Wyche K.P. Deep learning in airborne particulate matter sensing and surface plasmon resonance for environmental monitoring. *Atmosphere*. 2025. **16**. P. 359. https://doi.org/10.3390/atmos16040359.
14. Kukla O.L., Shirshov Yu.M., Biletskiy A.I. *et al*. Optimization of chromatic SPR sensor of gas environment based on registration of reflected beam color: Modeling and experiment. *SPQEO*. 2025. **28**. P. 374–382. https://doi.org/10.15407/spqeo28.03.374.
15. Selvi H., Capan I., Capan R., Acikbas Y. Sensing volatile organic compounds with CVD graphene: insights from quartz crystal microbalance and surface plasmon resonance studies. *J. Mater. Sci.: Mater. Electron*. 2024. **35**. P. 1268. https://doi.org/10.1007/s10854-024-13087-1.
16. Kostyukevych K.V., Khristosenko R.V., Shirshov Yu.M. *et al*. Multi-element gas sensor based on surface plasmon resonance: recognition of alcohols by using calixarene films. *SPQEO*. 2011. **14**. P. 313–320. https://doi.org/10.15407/spqeo14.03.313.
17. Riabchenko O.V., Kukla O.L., Fedchenko O.N. *et al*. SPR chromatic sensor with colorimetric registration for detection of gas molecules. *SPQEO*. 2023. **26**. P. 343–351. https://doi.org/10.15407/spqeo26.03.343.
18. Dorozinsky G.V., Lobanov M.V., Maslov V.P. Detection of methanol vapor by surface plasmon resonance method. *East.-Eur. J. Enterpr. Technol*. 2015. **4**(5). P. 4–7. https://doi.org/10.15587/1729-4061.2015.47079.
19. Dorozinsky G.V., Kachur N.V., Dorozinska H.V. *et al.* Highly-sensitive to *n*-hexane vapors SPR sensor with an additional ZnO layer. *Opt. Quant. Electron*. 2024. **56**. P. 1213. https://doi.org/10.1007/s11082-024-07085-0.
20. Fedorenko A.V., Bozhko K.M., Kachur N.V. *et al.* Optical and electrical properties of zinc oxide nanofilms deposited using the sol-gel method. *SPQEO*. 2024. **27**. P. 117–123. https://doi.org/10.15407/spqeo27.01.117.
21. Liu Z., He J., He S. Characterization and sensing of inert gases with a high-resolution SPR sensor. *Sensors*. 2020. **20**, No 11. P. 3295. https://doi.org/10.3390/s20113295.
22. Kruglenko I., Snopok B. Analyte-responsive metal–organic frameworks of polymer-stabilized silver nanoparticles for gas sensors. *Eng. Proc*. 2024. **82**. P. 64. https://doi.org/10.3390/ecsa-11-20458.
23. Hastings J.T., Guo J., Keathley P.D. *et al.* Optimal self-referenced sensing using long- and short-range surface plasmons. *Opt. Express*. 2007. **15**. P. 17661–17672. https://doi.org/10.1364/OE.15.017661.
24. Mitsushio M., Nagaura A., Yoshidome T., Higo M. Molecular selectivity development of Teflon AF1600-coated gold SPR-based glass rod sensor. *Prog. Org. Coat*. 2015. **79**. P. 62–67. https://doi.org/10.1016/j.porgcoat.2014.11.003.
25. Dorozinska H.V., Dorozinsky G.V., Maslov V.P. *et al.* Features of application of the additional nano layer of polytetrafluoroethylene in sensors based on surface plasmon resonance phenomenon. *Optoelectron. Semicond. Techn*. 2019. **54**. P. 88–95. https://doi.org/10.15407/iopt.2019.54.088.
26. Kostyukevych S.O., Koptiukh A.A., Kostyukevych K.V. *et al.* Improved surface plasmon resonance sensors with prism type of excitation on polymer basis. *Data Recording, Storage & Processing*. 2019. **21**. P. 183437. https://doi.org/10.35681/1560-9189.2019.21.3.183437.
27. Romanchuk V.V., Samoylov A.V., Venger Ye.F. *et al.* Modelling and research of the properties of plastic substrates of gas sensors based on surface plasmon resonance. *Optoelectron. Semicond. Techn*. 2024. **59**. P. 144–151. https://doi.org/10.15407/iopt.2024.59.144.
28. Grytsenko K., Kolomzarov Yu., Lytvyn P. *et al.* Variations of morphology of fluoropolymer thin films vs deposition conditions. *Surf. Topogr.: Metrol. Prop*. 2021. **9**. P. 5006. https://doi.org/10.1088/2051-672X/ac2a11.
29. Grytsenko K., Kolomzarov Yu., Lytvyn P. *et al.* Optical and mechanical properties of thin PTFE films deposited from a gas phase. *Macromol. Mater. Eng*. 2023. **308**. P. 2200617. https://doi.org/10.1002/mame.202200617.
30. Dorozinska H.V., Dorozinsky G.V., Maslov V.P. Promising method for determining the concentration of nanosized diamond powders in water suspensions. *Funct. Mater.* 2018. **25**. P. 158–164. https://doi.org/10.15407/fm25.01.158.
31. Börzsönyi A., Heiner Z., Kalashnikov M.P. *et al.* Dispersion measurement of inert gases and gas mixtures at 800 nm. *Appl. Opt.* 2008. **47**. P. 4856–4863. https://doi.org/10.1364/AO.47.004856.
32. Meng Q.Q., Zhao X., Lin C.Y. *et al.* Figure of merit enhancement of a surface plasmon resonance sensor using a low-refractive-index porous silica film. *Sensors* (Basel). 2017. **17**, No 8. P. 1846. https://doi.org/10.3390/s17081846.
33. Ozdemir S.K., Turhan-Sayan G. Temperature effects on surface plasmon resonance: Design considerations for an optical temperature sensor. *J. Light. Technol*. 2003. **21**. P. 805–814. https://doi.org/10.1109/JLT.2003.809552.

34. Bruggeman D.A.G. Berechnung verschiedener physikalischer Konstanten von heterogenen Substanzen. I. Dielektrizitätskonstanten und Leitfähigkeiten der Mischkörper aus isotropen Substanzen. *Annalen der Physik*. 1935. **416**, No 7. P. 636–664. https://doi.org/10.1002/andp.19354160705.
35. Schott F2 Glass. SONGHAN Plastic Technology Co., Ltd. https://www.lookpolymers.com/pdf/Schott-F2-Glass.pdf (Accessed 30 May, 2026).
36. Mahesh Kumar R., Rajini N., Mayandi K. *et al.* Investigation on thermal properties of Styrene Acrylonitrile (SAN) matrix with Polytetrafluroethylene (PTFE) particle reinforced composites. *IOP Conf. Ser.: Mater. Sci. Eng.* 2018. **390**. P. 012003. https://doi.org/10.1088/1757-899X/390/1/012003.

Authors and CV

Glib Dorozinsky, PhD in Engineering Sciences, senior researcher of the Department of Sensor Systems, V. Lashkaryov Institute of Semiconductor Physics, NAS of Ukraine. Author of more than 60 scientific publications, 40 patents, and co-author of 2 collective monographs. The area of his scientific interests includes the physics of surfaces, development and design of surface plasmon resonance based sensors for application in different fields like medicine, pharmacology, industry, and ecology. http://orcid.org/0000-0002-7881-2493

Yuriy V. Kolomzarov, PhD, Senior Scientist at the V. Lashkaryov Institute of Semiconductor Physics, NAS of Ukraine, Department of Optoelectronics. Authored over 40 publications. Scientific interests includes physics and technology of metal-organic materials, hybrid structures with metal nanoparticles and devices (gas sensors, organic-inorganic light-emitted structures, *etc.*). E-mail: kolomzarov@isp.kiev.ua, http://orcid.org/0000-0002-6314-9529

K.P. Grytsenko, PhD in Materials Science at the Kharkov Institute of Monocrystals, 2000. Since 1999 he is working at the V. Lashkaryov Institute of Semiconductor Physics, NAS of Ukraine, when he obtained scientific rank of Senior Research Scientist in 2004. Area of his scientific activity includes the development of both compounds and deposition technology for production of hybrid nanocomposite thin films for various optoelectronics applications, including optical memory, optical sensors and biotechnology. https://orcid.org/0000-0002-2956-3654

Vladyslav Romanchuk, MSc (2022), PhD student at the V. Lashkaryov Institute of Semiconductor Physics, NAS of Ukraine. His research interests focus on the development of optical sensors based on the surface plasmon resonance phenomenon as well as their implementation for biological and medical needs.
E-mail: vladyslav.v.romanchuk@gmail.com,
https://orcid.org/0009-0001-2254-4485

Hanna Dorozinska, PhD in Engineering Sciences, Associate Professor of the Department of Information and Measuring Technologies (IMT) at the Faculty of Robotics and Instrumentation Engineering, National Technical University of Ukraine “Igor Sikorsky Kyiv Polytechnic Institute”. Author of more than 40 scientific publications, 10 patents, and co-author of 1 collective monograph. The area of her scientific interests includes optics, the application of surface plasmon resonance based sensors for applications in different fields like medicine, pharmacology, industry, and ecology.
E-mail: annakushnir30@ukr.net,
http://orcid.org/0000-0002-9352-3761

Tamara P. Doroshenko, Researcher of the Department of Biochemosensory Sciences, V. Lashkaryov Institute of Semiconductor Physics, NAS of Ukraine. Author of more than 50 scientific publications and 7 patents. The area of her scientific interests includes the development of technologies and methods for the deposition of nanocomposite and multilayer thin films of metals, semiconductors, and organic dyes, with their subsequent use in nanosensors and nanoplasmonics, and research of their optical and photophysical properties.
E-mail: tompavl54@gmail.com,
https://orcid.org/0000-0002-6602-6356

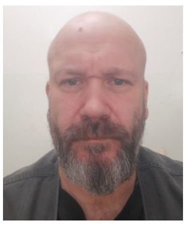

Anton V. Samoylov, PhD, Head of the research group on the development of sensors based on surface plasmon resonance, Department of Sensor Systems, V. Lashkaryov Institute of Semiconductor Physics, NAS of Ukraine. He is the author of more than 84 scientific publications. The area of his scientific interests includes optical sensors, surface plasmon resonance, achromatic and super-achromatic zero-order waveplates.
E-mail: samoylov_anton@ukr.net,
https://orcid.org/0000-0001-5149-693X

Andrii A. Korchovyi, PhD in Physics and Mathematics, Senior Researcher at the Laboratory for scanning probe microscopy, V. Lashkaryov Institute of Semiconductor Physics, NAS of Ukraine. Authored over 100 publications. The area of his scientific interests includes atomic force microscopy, physical and chemical properties of semiconductor materials, and nanostructures for modern micro- and nano-electronics. E-mail: akorchovyi@gmail.com, https://orcid.org/0000-0002-8848-7049

Oksana M. Strilchuk, PhD in Physics and Mathematics, Senior Researcher at the Department of Sensor Systems, V. Lashkaryov Institute of Semiconductor Physics, NAS of Ukraine. Author of more than 50 scientific publications. The area of her scientific interests includes optical sensors, solid-state luminescent materials, light-emitting devices and structures, thin films, quantum dots and modification of physical properties of solids by interacting with laser, electron and γ-radiation.
E-mail: ostrilchuk@gmail.com
https://orcid.org/0000-0002-5141-3230

Roman V. Khrystosenko, PhD, Senior Research Fellow of the research group on the development of sensors based on surface plasmon resonance, Department of Sensor Systems, V. Lashkaryov Institute of Semiconductor Physics, NAS of Ukraine. Author of more than 80 scientific publications. The area of his scientific interests includes optical sensors based on surface plasmon resonance phenomenon. E-mail: khristosenko@ukr.net, https://orcid.org/0000-0002-0440-2651

Authors' contributions

Dorozinsky G.V.: project administration, investigation, methodology, writing – review & editing.
Kolomzarov Yu.V.: formal analysis, resources, synthesis, writing – review & editing.
Grytsenko K.P.: methodology, conceptualization.
Romanchuk V.V.: investigation, visualization.
Dorozinska H.V.: visualization, methodology, writing – original draft, writing – review & editing.
Doroshenko T.P.: methodology, formal analysis, resources, synthesis, writing – review & editing.
Korchovyi A.A.: investigation, formal analysis, resources, writing – review & editing.
Samoylov A.V.: investigation, supervision.
Strilchuk O.M.: investigation, visualization.
Khrystosenko R.V.: investigation, methodology.

Вплив матеріалу підкладки на чутливість ППР сенсора з політетрафторетиленовим покриттям до інертного газу

Г.В. Дорожинський, Ю.В. Коломзаров, К.П. Гриценко, В.В. Романчук, Г.В. Дорожинська, Т.П. Дорошенко, А.В. Самойлов, А.А. Корчовий, О.М. Стрільчук, Р.В. Христосенко

Анотація. Досліджено вплив матеріалу підкладки у поєднанні з шаром політетрафторетилену (PTFE) на чутливість оптичних сенсорів на основі поверхневого плазмонного резонансу (ППР) у геометрії Кречмана. Експерименти проведено при фіксованій довжині хвилі збудження поверхневих плазмонів з використанням шару золота, що підтримує плазмони. Сенсорні елементи випробувано шляхом циклічного витіснення навколишнього повітря інертним гелієм у проточній комірці. Порівняльний аналіз характеристик ППР сенсорів на підкладках, виготовлених з оптичного скла F1 та стирол-акрилонітрильного (SAN) полімеру, проведено як за наявності, так і за відсутності шару PTFE на поверхні плівки Au. Було встановлено, що заміна скляної підкладки полімером SAN приводить до збільшення чутливості з 45,8 до 48,1 град/RIU через зменшення показника заломлення; однак це подвоює показник якості (FOM) з 26,2 до 50,1 RIU^{-1}. Застосування PTFE покриття для обох типів сенсорів привело до збільшення чутливості: з 45,8 до 74,4 град/RIU для скляної підкладки та з 48,1 до 52,1 град/RIU для полімерної підкладки. Окрім підвищеної чутливості, використання полімерного матеріалу дозволяє знизити вартість кінцевого продукту та спростити етапи прецизійної обробки поверхні. Додатковою перевагою застосування полімерних підкладок є звуження резонансних кривих, що значно підвищує точність реєстрації кута резонансу.

Ключові слова: сенсор, поверхневий плазмонний резонанс, підкладка, політетрафторетилен, стирол-акрилонітрил, гелій, чутливість, коефіцієнт якості.